

# A Six Degrees-of-Freedom Vibration Isolation Platform Supported by a Hexapod of Quasi-Zero-Stiffness Struts

Jiayi Zhou<sup>1</sup>

College of Mechanical and Vehicle Engineering,  
Hunan University,  
Changsha 410082, China  
e-mail: jxizhou@hnu.edu.cn

Kai Wang

College of Mechanical and Vehicle Engineering,  
Hunan University,  
Changsha 410082, China  
e-mail: wangkai@hnu.edu.cn

Daolin Xu

College of Mechanical and Vehicle Engineering;  
State Key Laboratory of Advanced Design and  
Manufacturing for Vehicle Body,  
Changsha 410082, China  
e-mail: dlxu@hnu.edu.cn

Huajiang Ouyang

School of Engineering,  
University of Liverpool,  
Liverpool L69 3GH, UK  
e-mail: h.ouyang@liverpool.ac.uk

Yingli Li

School of Traffic and Transportation Engineering,  
Central South University,  
Changsha 410082, China  
e-mail: liyingli@hnu.edu.cn

*A platform supported by a hexapod of quasi-zero-stiffness (QZS) struts is proposed to provide a solution for low-frequency vibration isolation in six degrees-of-freedom (6DOFs). The QZS strut is developed by combining a pair of mutually repelling permanent magnets in parallel connection with a coil spring. Dynamic analysis of the 6DOFs QZS platform is carried out to obtain dynamic responses by using the harmonic balance method, and the vibration isolation performance in each DOF is evaluated in terms of force/moment transmissibility, which indicates that the QZS platform perform a good function of low-frequency vibration isolation within broad bandwidth, and has notable advantages over its linear counterpart in all 6DOFs. [DOI: 10.1115/1.4035715]*

## 1 Introduction

The technique of passive vibration isolation is widely applied to mitigate the transmission of vibratory forces to the base or disturbances to the payload in a large number of engineering areas [1]. However, the traditional passive isolator with linear stiffness is effective only when its natural frequency is well below the excitation frequency. For very low excitation frequency, a soft resilient element is needed to lower its natural frequency, but it

would experience excessive static deflection leading to degradation and even failure of the system. Therefore, how to achieve very low-frequency isolation is still a popular and open research topic.

Recently, one category of QZS isolator [2] has attracted more and more attention, due to its high static but low dynamic stiffness. The key issue of designing a QZS isolator is to establish compact and reliable negative-stiffness (NS) mechanisms. There exist many potential design concepts of NS mechanisms: oblique springs [3–5], oblique linkages connecting horizontal springs [6], cam-roller-spring mechanisms [7], bi-stable structures [8], scissor-like platforms [9], and magnetic springs [10,11]. Nearly all the theoretical and experimental studies show their capabilities in low-frequency vibration isolation and advantages over their linear counterparts.

Nevertheless, most QZS isolators are developed for vibration isolation in the vertical translational direction. In practice, excitations acting on the payload are aroused from the on-board machine in multiple directions rather than sole direction. To deal with multidirection excitations, one possible solution is to arrange multiple QZS isolators in the excitation directions, but this is not an ideal method, because of the requirement on structural simplicity and space-restrictive packaging. Therefore, a multi-DOF QZS isolator with compact and simple mechanisms or structures is needed to provide a feasible solution to this issue.

Stewart platforms, using six variable active legs to connect a movable plate to a fixed base, have been widely used as 6DOFs motion generators (e.g., flight simulator) [12], 6DOFs parallel manipulators [13], and active vibration isolators [14]. Considering the advantages of Stewart platforms in structural compactness and simplicity and 6DOFs positioning capabilities, replacing the legs by QZS struts to form a purely passive 6DOFs-QZS vibration isolation platform would be a potential solution to multidirection vibration isolation [15,16], with the characteristics of no-power consumption and reliability.

The aim of the present work is to develop a QZS strut as the leg of a Stewart platform to construct a 6DOFs-QZS vibration isolation platform. The QZS strut is devised by combining a pair of mutually repelling permanent magnets in parallel connection with a coil spring. To derive concise kinematics and dynamic relationships, a cubic configuration of the arrangement of struts is adopted following Geng and Haynes [14]. The effectiveness of vibration isolation is estimated in terms of force/moment transmissibility in all six directions, and compared with its linear counterpart to reveal its advantages.

## 2 Conceptual Model of the Six Degrees-of-Freedom Quasi-Zero-Stiffness Platform

The schematic diagram of the 6DOFs-QZS vibration isolation platform is shown in Fig. 1(a). The payload plate is supported by six QZS struts. A payload, assumed to be a rigid cylinder, is fixed on the top plate. The symmetric axis of the payload coincides with the vertical axis of the whole platform. Connecting points and QZS struts are marked by numbers without and with circles, respectively. The origin of the coordinate system is located on the centroid of the payload (including the payload plate).

Quasi-zero-stiffness struts are arranged in a cubic configuration, as shown in Fig. 1(b), and the adjacent pair of struts are perpendicular to each other. Physical models of connecting points are not depicted in this schematic diagram. Theoretically, they are assumed to be ideal ball joints, and thus, the bending of the strut can be neglected, and only the axial deformation is considered.

The schematic diagram of the magnetic QZS strut is shown in Fig. 1(c). Inner ring permanent magnet (5) with inner radius  $R$  is fixed on rod (1) by two locking nuts (10). The rod can only slide along the axial direction guided by two linear bearings (2). Outer ring permanent magnet (4) is fixed on sleeve (3) by four symmetrically distributed fastening bolts (11). Both permanent magnets

<sup>1</sup>Corresponding author.

Contributed by the Technical Committee on Vibration and Sound of ASME for publication in the JOURNAL OF VIBRATION AND ACOUSTICS. Manuscript received July 23, 2016; final manuscript received January 3, 2017; published online April 18, 2017. Assoc. Editor: Patrick S. Keogh.

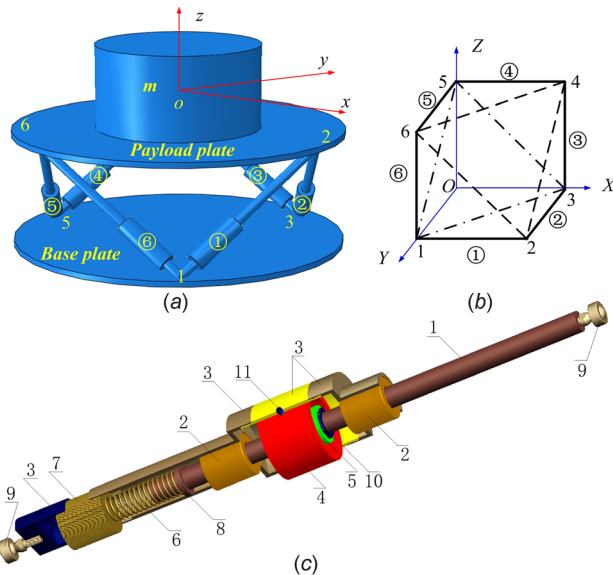


**Fig. 1** Schematic diagram of the 6DOFs-QZS vibration isolation platform. (a) three-dimensional model, (b) arrangement of connecting points and QZS struts, and (c) QZS strut at the equilibrium position.

have identical width  $l$  and height  $h$ , as well as the same axial magnetization direction, and the air gap between the two magnets is  $g$ .

Under a payload, the strut arrives at the static equilibrium position, and the inner magnet (5) aligns in parallel with the outer magnet (4). This configuration can serve as a radial permanent magnet bearing with mutually repelling feature, which has radial stable positive stiffness but axial negative stiffness near the equilibrium position [17]. Therefore, a pair of permanent magnets with mutually repelling feature can be utilized as a negative-stiffness mechanism [10,11] to construct a QZS strut.

A coil spring (6) with stiffness  $k_v$  acts as the positive stiffness element to neutralize the negative stiffness, and thus, achieve a stable QZS stiffness. A chuck (8) is fixed on one end of rod (1) to lock the coil spring. To handle different amounts of the payload, a precompression adjustor (7) with screw threads is setup between two segments of the sleeve (3). To assemble a vibration isolation platform by using the QZS struts, ball joints (9) are set at two ends of the strut. The stiffness of the rod is much larger than that of coil spring so that the rod is assumed to be rigid.

When an additional axial force  $f$  is acting on the rod along the axial direction, a resultant axial deformation  $x$  will occur. By using the nondimensional terms  $\bar{x} = x/R$  and  $\bar{f} = f/(k_v R)$ , the relationship between  $\bar{f}$  and  $\bar{x}$  can be expressed as

$$\bar{f} = \bar{x} - \bar{f}_m = \bar{x} - \alpha[2\bar{\phi}(\bar{x}) - \bar{\phi}(\bar{x} + \bar{h}) - \bar{\phi}(\bar{x} - \bar{h})] \quad (1)$$

where  $\bar{f}_m$  is the repelling magnetic force [18], and

$$\bar{\phi}(a) = (2\bar{l} + \bar{g})\tan^{-1}\frac{2\bar{l} + \bar{g}}{a} - 2(\bar{l} + \bar{g})\tan^{-1}\frac{\bar{l} + \bar{g}}{a} + g\tan^{-1}\frac{\bar{g}}{a} - \frac{a}{2}\left\{\ln\left[(2\bar{l} + \bar{g})^2 + a^2\right] - 2\ln(\bar{l} + \bar{g})^2 + \ln(\bar{g}^2 + a^2)\right\} \quad (2)$$

and  $\alpha = (\sigma^2 R_m)/(\mu_0 k_v)$ , where  $\sigma = \mathbf{J} \cdot \mathbf{n}$  is magnetic pole surface density,  $\mathbf{J}$  is the magnetic polarization vector, and  $\mathbf{n}$  is the unit normal vector;  $\mu_0$  is the permeability of the vacuum;  $R_m = R + l + g/2$  is average radius of the inner and outer permanent magnets. Let  $d\bar{f}/d\bar{x} = 0$  at  $\bar{x} = 0$ , and one can get the zero-stiffness condition

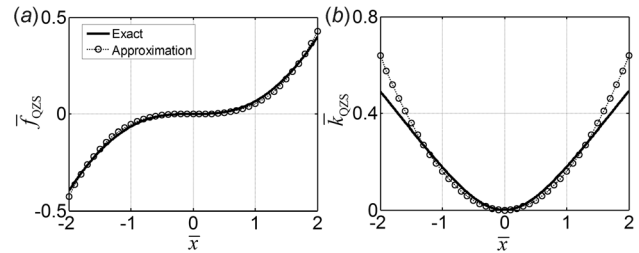


**Fig. 2** (a) Force and (b) stiffness versus displacement relations of the QZS strut

$$\frac{1}{\alpha_{QZS}} = \frac{4\bar{h}^2}{\bar{h}^2 + (\bar{l} + \bar{g})^2} + \ln\frac{[(2\bar{l} + \bar{g})^2 + \bar{h}^2](\bar{g}^2 + \bar{h}^2)}{(2\bar{l} + \bar{g})^2 \bar{g}^2} \quad (3)$$

By substituting the above equation into Eq. (1), the restoring force of the QZS strut can be given by

$$\bar{f}_{QZS} = \bar{x} - \alpha_{QZS}[2\bar{\phi}(\bar{x}) - \bar{\phi}(\bar{x} + \bar{h}) - \bar{\phi}(\bar{x} - \bar{h})] \quad (4)$$

To simplify the following dynamic analysis of the platform, the restoring force is approximated as a polynomial to achieve a concise expression with enough accuracy, as illustrated in Fig. 2, when  $\alpha_{QZS} = 0.1451$ ,  $\bar{g} = 1$ ,  $\bar{h} = 5$ ,  $\bar{l} = 2$ , and  $R = 10$  mm. It can be seen that the third-order polynomial fitting matches the exact relationship well, and thus, the restoring force  $\bar{f}_{QZS}$  can be approximated as

$$\bar{f}_{QZS}^a(\bar{x}) = \gamma\bar{x}^3 \quad (5)$$

### 3 Transmissibility of the Six Degrees-of-Freedom Quasi-Zero-Stiffness Platform

The equations of motion of the QZS platform system can be given by

$$\mathbf{M}\ddot{\mathbf{u}} + \mathbf{K}\mathbf{u} = \mathbf{F} \quad (6)$$

where

$$\mathbf{M} = \text{diag}[m, m, m, I_x, I_y, I_z], \quad \mathbf{u} = \{x, y, z, \theta_x, \theta_y, \theta_z\}^T,$$

$$\mathbf{K} = \mathbf{0}, \quad \mathbf{F} = \mathbf{F}_t - \mathbf{F}_R$$

$$\mathbf{F}_R = \{F_x(\mathbf{u}), F_y(\mathbf{u}), F_z(\mathbf{u}), M_x(\mathbf{u}), M_y(\mathbf{u}), M_z(\mathbf{u})\}^T$$

$$\mathbf{F}_t = \mathbf{F}_0 \cos \omega t = \{F_{x0}, F_{y0}, F_{z0}, M_{x0}, M_{y0}, M_{z0}\}^T \cos \omega t \quad (7)$$

where  $\mathbf{F}_R$  is the restoring force of the QZS platform as a function of displacement  $\mathbf{u}$ , which can be obtained by static analysis of the platform;  $m$  is the mass of the payload (including payload plate);  $I$  is the moment of inertia of the payload; All the excitations are harmonic, and  $\mathbf{F}_0$  is the amplitude of the excitation. Since there is only a cubic term in the restoring force of the QZS strut (Eq. (5)), the linear term in the equations of motion is zero, and thus,  $\mathbf{K} = \mathbf{0}$ .

By using the following nondimensional terms

$$\bar{x} = \frac{x}{R}, \quad \omega_{nz} = \sqrt{\frac{2k_v}{m}}, \quad \bar{t} = \omega_{nz} t, \quad \Omega = \frac{\omega}{\omega_{nz}}, \quad (8)$$

$$\bar{F} = \frac{F}{2k_v R}, \quad \bar{M} = \frac{M}{2k_v R^2 I}, \quad \bar{I} = \frac{I}{mR^2}$$

and including an equivalent linear viscous damping to account for dissipative terms, the equations of motion can be rewritten as

$$\ddot{\bar{\mathbf{u}}} + 2\zeta\dot{\bar{\mathbf{u}}} + \bar{\mathbf{K}}\bar{\mathbf{u}} = \bar{\mathbf{F}} \quad (9)$$

where  $(\cdot)' = d(\cdot)/d\bar{t}$ , and

$$\begin{aligned} \bar{\mathbf{u}} &= \{\bar{x}, \bar{y}, \bar{z}, \theta_x, \theta_y, \theta_z\}^T, \quad \zeta = \text{diag}[\zeta_1, \zeta_2, \zeta_3, \zeta_4, \zeta_5, \zeta_6], \\ \bar{\mathbf{K}} &= \mathbf{0}, \quad \bar{\mathbf{F}} = \bar{\mathbf{F}}_f - \bar{\mathbf{F}}_R \end{aligned} \quad (10)$$

The first approximation of the primary resonance is obtained by using the Harmonic Balance method. The fundamental responses are assumed to be

$$\begin{aligned} \bar{\mathbf{u}} &= \bar{\mathbf{U}}_1 \cos \Omega \bar{t} + \bar{\mathbf{U}}_2 \sin \Omega \bar{t} \\ \bar{\mathbf{U}}_1 &= \{X_1, Y_1, Z_1, \Theta_{x1}, \Theta_{y1}, \Theta_{z1}\}^T, \\ \bar{\mathbf{U}}_2 &= \{X_2, Y_2, Z_2, \Theta_{x2}, \Theta_{y2}, \Theta_{z2}\}^T \end{aligned} \quad (11)$$

Substituting Eq. (11) into Eq. (9) results in

$$\begin{aligned} -\Omega^2(\bar{\mathbf{U}}_1 \cos \Omega \bar{t} + \bar{\mathbf{U}}_2 \sin \Omega \bar{t}) - 2\Omega \zeta(\bar{\mathbf{U}}_1 \sin \Omega \bar{t} - \bar{\mathbf{U}}_2 \cos \Omega \bar{t}) \\ + \bar{\mathbf{F}}_R(\bar{\mathbf{u}}) = \bar{\mathbf{F}}_0 \cos \Omega \bar{t} \end{aligned} \quad (12)$$

By ignoring the high-order harmonic terms,  $\bar{\mathbf{F}}_R(\bar{\mathbf{u}})$  can be approximated as

$$\bar{\mathbf{F}}_R(\bar{\mathbf{u}}) \approx \bar{\Gamma}_{R1} \cos \Omega \bar{t} + \bar{\Gamma}_{R2} \sin \Omega \bar{t} \quad (13)$$

where  $\bar{\Gamma}_{R1}$  and  $\bar{\Gamma}_{R2}$  are functions of  $\bar{\mathbf{U}}_1$  and  $\bar{\mathbf{U}}_2$ , and independent of time  $\bar{t}$ . By equating coefficients of  $\cos \Omega \bar{t}$  and  $\sin \Omega \bar{t}$  in Eq. (12), the amplitude-frequency equations can be given by

$$\begin{cases} -\Omega^2 \bar{\mathbf{U}}_1 + 2\Omega \zeta \bar{\mathbf{U}}_2 + \bar{\Gamma}_{R1} = \bar{\mathbf{F}}_0 \\ -\Omega^2 \bar{\mathbf{U}}_2 - 2\Omega \zeta \bar{\mathbf{U}}_1 + \bar{\Gamma}_{R2} = 0 \end{cases} \quad (14)$$

The above equation are third-order nonlinear algebraic equations of displacement amplitudes  $\bar{\mathbf{U}}_1$  and  $\bar{\mathbf{U}}_2$ , which can be solved numerically.

The forces/moments transmitted to the base can be given by

$$\begin{aligned} \bar{\mathbf{F}}_T &= 2\zeta \bar{\mathbf{u}}' + \bar{\mathbf{F}}_R(\bar{\mathbf{u}}) \\ &\approx -2\Omega \zeta(\bar{\mathbf{U}}_1 \sin \Omega \bar{t} - \bar{\mathbf{U}}_2 \cos \Omega \bar{t}) + (\bar{\Gamma}_{R1} \cos \Omega \bar{t} + \bar{\Gamma}_{R2} \sin \Omega \bar{t}) \\ &= (\bar{\Gamma}_{R1} + 2\Omega \zeta \bar{\mathbf{U}}_2) \cos \Omega \bar{t} + (\bar{\Gamma}_{R2} - 2\Omega \zeta \bar{\mathbf{U}}_1) \sin \Omega \bar{t} \\ &\triangleq (\bar{\mathbf{F}}_0 + \Omega^2 \bar{\mathbf{U}}_1) \cos \Omega \bar{t} + \Omega^2 \bar{\mathbf{U}}_2 \sin \Omega \bar{t} \end{aligned} \quad (15)$$

The force/moment transmissibility is defined as the ratio of the amplitude of the transmitted force/moment to that of the excitation in the form of decibel

$$\mathbf{T}(i) = 20 \log_{10} \frac{\sqrt{[\bar{\mathbf{F}}_0(i) + \Omega^2 \bar{\mathbf{U}}_1(i)]^2 + [\Omega^2 \bar{\mathbf{U}}_2(i)]^2}}{\bar{\mathbf{F}}_0(i)} \quad (i = 1 \sim 6) \quad (16)$$

where  $\mathbf{T} = \{T_{F_x}, T_{F_y}, T_{F_z}, T_{M_x}, T_{M_y}, T_{M_z}\}^T$  represents transmissibility along each direction, which is utilized to evaluate the vibration isolation performance in each DOF.

The analytical transmissibility is verified by a numerical analysis, which are defined in statistic form as the ratio of root-mean-square (RMS) of the transmitted force/moment to that of the excitation [7], i.e.,

$$T_{NS} = 20 \log_{10} \left( \frac{\text{RMS}[\bar{\mathbf{F}}_T(\bar{t}_i)]}{\text{RMS}[\bar{\mathbf{F}}(\bar{t}_i)]} \right) \quad (17)$$

where  $\bar{\mathbf{F}}_T(\bar{t}_i)$  and  $\bar{\mathbf{F}}(\bar{t}_i)$  are time histories of the transmitted force/moment and the excitation in each DOF, respectively, and  $\bar{\mathbf{F}}_T(\bar{t}_i)$  is calculated based on the responses which is obtained by solving the equations of motion using Runge-Kutta algorithm.

To illustrate the vibration isolation performance, parameters of the platform listed in Table 1 are used, where  $\bar{L}$  is the length of

**Table 1 Parameters of the platform**

Parameter	$\bar{L}$	$\bar{Z}_c$	$\bar{I}_x$	$\bar{I}_y$	$\bar{I}_z$	$m$
Value	35	5	57.33	57.33	98	30 kg

**Table 2 Amplitudes of the excitations ( $\times 10^{-5}$ ) and damping ratios**

Parameter	$\bar{F}_{x0}$	$\bar{F}_{y0}$	$\bar{F}_{z0}$	$\bar{M}_{x0}$	$\bar{M}_{y0}$	$\bar{M}_{z0}$	$\zeta_i, i = 1 \sim 6$
Value	60.773	60.773	60.773	1.4840	1.4840	0.86820	0.1

the strut, and  $\bar{Z}_c$  is the distance from the centroid of the payload to the center of the payload plate. The amplitudes of excitation forces are selected as  $\eta = 1\%$  of the payload weight (later on  $\eta = 10\%$  will be considered), and three forces acting at an off-center location ( $e = 10\%$  of the radius of gyration with respect to  $z$  axis of the payload) yield three excitation moments, which are summarized in Table 2. Note that the actual damping needs to be determined by experimental tests on a physical prototype of this platform. To reveal the effectiveness of this new platform, an equivalent constant viscous damping is adopted based on our previous experimental tests on different kinds of QZS isolators [5–7]. Additionally, the effects of damping on transmissibility will be discussed in Sec. 4.

Transmissibility in 6DOFs compared with its linear counterpart is depicted in Fig. 3. Note that the linear counterpart is constructed by removing all negative-stiffness mechanisms (permanent magnets). Analytical results are validated by numerical simulations with both forward and backward frequency sweeps. There exists a very good agreement between the analytical and numerical results. Jump phenomenon is not observed due to the weak steady-state oscillations under small excitations and comparatively heavy damping.

For the linear system, there are two peaks in two in-plane translational and two out-of-plane rotational DOFs due to the stiffness coupling effects, and antiresonance of  $T_{M_x}$  occurs at a low frequency. In contrast, for the QZS system, no resonant peak is observed on each transmissibility curve of three translational DOFs, and a single slight resonant peak at ultra-low frequencies occurs on each curve of three rotational DOFs.

Most importantly, the ultra-low stiffness leads to a super vibration isolation performance. It is obvious that almost in the whole frequency range the QZS platform is effective for vibration isolation in all 6DOFs, except only at ultra-low frequencies. The transmissibility of the QZS platform is much lower than its linear counterpart; especially for rotational DOFs the advantage is more notable, which reveals superiorities of the QZS platform over its linear counterpart.

#### 4 Effects of Damping and Excitation Amplitude

Generally, transmissibility is dependent on the level of damping and excitation. The multivalued feature of nonlinear dynamic systems also can be affected by these two parameters. Effects of damping on transmissibility are depicted in Fig. 4, where two cases of the light ( $\zeta = 0.01$ ) and heavy ( $\zeta = 0.1$ ) damping are considered. Only transmissibility of  $T_{F_z}$  and  $T_{M_z}$  are presented for the sake of brevity, and the effects of damping on transmissibility in other DOFs are similar to those presented in Fig. 4.

In the case of light damping, the nonlinear multivalued characteristics are activated. There exist three solutions of transmissibility  $T_{F_z}$  in a certain frequency range, among which two solutions are stable, and the third one is unstable, as illustrated in Fig. 4(a). For  $T_{M_z}$ , a *bubble* (named after its shape), namely, a closed detached resonance curve, is formed (Fig. 4(b)). Furthermore, the stiffness coupling effects of the QZS system are also activated in

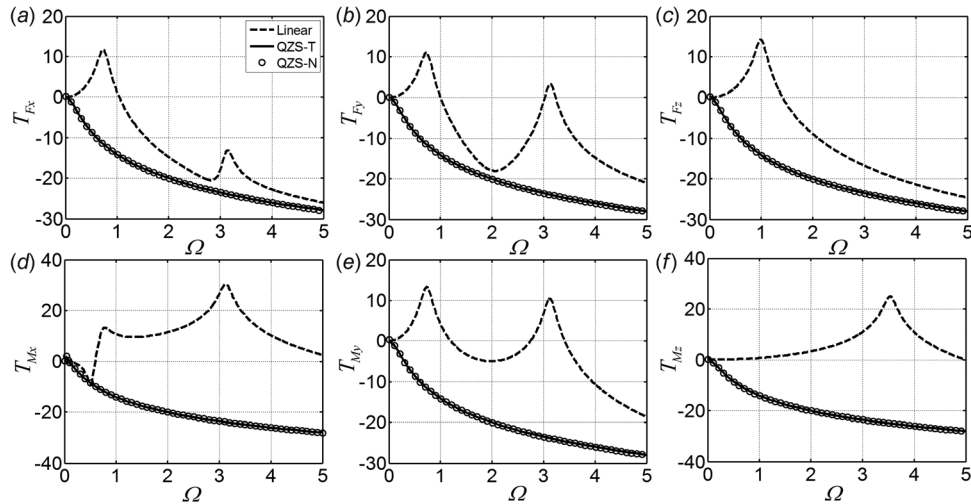


**Fig. 3** Transmissibility of the QZS platform compared with its linear counterpart: (a)  $T_{F_x}$ , (b)  $T_{F_y}$ , (c)  $T_{F_z}$ , (d)  $T_{M_x}$ , (e)  $T_{M_y}$ , and (f)  $T_{M_z}$ . Solid lines and dashed lines denote theoretical results of the QZS system (QZS-T) and its linear counterpart, respectively, and hollow cycles represent numerical results of the QZS system (QZS-N).

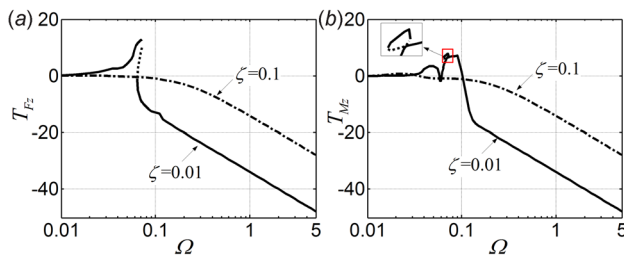


**Fig. 4** Effects of damping on transmissibility (a)  $T_{F_z}$  and (b)  $T_{M_z}$ , when  $\eta = 1\%$ . Dashed lines denote unstable solutions in the case of  $\zeta = 0.01$ .

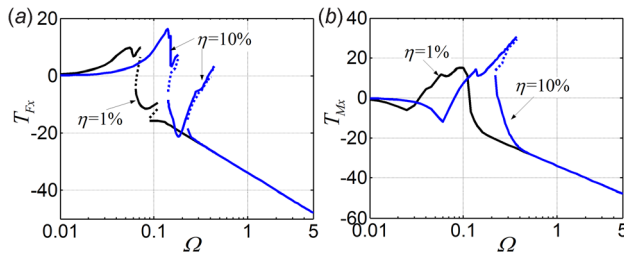


**Fig. 5** Effects of excitation amplitude on transmissibility (a)  $T_{F_x}$  and (b)  $T_{M_x}$ , when  $\zeta = 0.01$ . Dashed lines denote unstable solutions.

such situations, resulting in two peaks on transmissibility curves of the rotational DOF, as shown in Fig. 4(b). Therefore, heavy damping can be utilized to suppress resonance, mitigate the stiffness coupling effects, and avoid complicated dynamic behaviors, such as multivalued solutions.

However, due to the inherent characteristics of vibration isolation system, heavy damping would degrade the vibration isolation effectiveness in high-frequency range. Fortunately, both resonances and multiple solutions only appear in the very low-frequency range under light damping. Thus, even for light damping, such as  $\zeta = 0.01$ , the QZS platform still perform an excellent function of vibration isolation with high effectiveness and broad bandwidth.

Effects of excitation amplitudes on transmissibility, e.g.,  $T_{F_x}$  and  $T_{M_x}$ , are illustrated in Fig. 5. Two levels of the excitation, namely  $\eta = 1\%$  and  $\eta = 10\%$ , are considered. Obviously,

increasing excitation enlarges the peak of transmissibility and leads to a shift of the peak into higher-frequency range, and thus, the multivalued frequency range becomes broader, and jump phenomenon is more obvious. However, those unfavorable events also occur in low-frequency range, which has an insignificant influence on vibration isolation performance.

## 5 Conclusions

A 6DOFs-QZS platform is proposed, and its vibration isolation performances are investigated. It is found that the QZS platform is effective nearly in the whole range of frequency under small excitation and comparatively heavy damping, and it has a big advantage over its linear counterpart in all 6DOFs. Both damping level and excitation amplitude can influence transmissibility. Heavy damping suppresses resonances and appearances of multiple solutions, but degrades isolation performance in the effective frequency range. Peak transmissibility increases, and the multivalued frequency bandwidth becomes broader, as the excitation amplitude increases. Fortunately, the degradation of vibration isolation performance occurs only in very low-frequency range. Therefore, this 6DOFs-QZS platform can perform very well in low-frequency vibration isolation, even under relatively large excitations and light damping.

## Acknowledgment

We would like to appreciate Professor Xinong Zhang of Xi'an Jiaotong University for his helpful advice. This research work was supported by National Natural Science Foundation of China (Grant Nos. 11572116 and 11402082), Natural Science Foundation of Hunan Province (Grant No. 2016JJ3036), and Fundamental Research Funds for the Central Universities. This work is carried out during the first author's visit to the University of Liverpool.

## References

- [1] Rivin, E. I., 2003, *Passive Vibration Isolation*, American Society of Mechanical Engineers Press, New York.
- [2] Alabuzhev, P., Gritchin, A., Kim, L., Migirenko, G., Chon, V., and Stepanov, P., 1989, *Vibration Protecting and Measuring System With Quasi-Zero Stiffness*, Taylor & Francis Group, New York.
- [3] Cao, Q., Wiercigroch, M., Pavlovskaia, E. E., Grebogi, C., Thompson, T., and Michael, J., 2006, "Archetypal Oscillator for Smooth and Discontinuous Dynamics," *Phys. Rev. E*, **74**(4), p. 046218.
- [4] Abolfathil, A., Brennan, M. J., Waters, T. P., and Tang, B., 2015, "On the Effects of Mistuning a Force-Excited System Containing a Quasi-Zero-Stiffness Vibration Isolator," *ASME J. Vib. Acoust.*, **137**(4), p. 044502.

- [5] Xu, D., Zhang, Y., Zhou, J., and Lou, J., 2014, "On the Analytical and Experimental Assessment of Performance of a Quasi-Zero-Stiffness Isolator," *J. Vib. Control*, **20**(15), pp. 2314–2325.
- [6] Xu, D., Yu, Q., Zhou, J., and Bishop, S. R., 2013, "Theoretical and Experimental Analyses of a Nonlinear Magnetic Vibration Isolator With Quasi-Zero-Stiffness Characteristic," *J. Sound Vib.*, **332**(14), pp. 3377–3389.
- [7] Zhou, J., Wang, X., Xu, D., and Bishop, S., 2015, "Nonlinear Dynamic Characteristics of a Quasi-Zero Stiffness Vibration Isolator With Cam-Oller-Pring Mechanisms," *J. Sound Vib.*, **346**, pp. 53–69.
- [8] Fulcher, B., Shahan, D., Haberman, M., Seepersad, C. C., and Wilson, P., 2014, "Analytical and Experimental Investigation of Buckled Beams as Negative Stiffness Elements for Passive Vibration and Shock Isolation Systems," *ASME J. Vib. Acoust.*, **136**(3), p. 031009.
- [9] Sun, X., and Jing, X., 2015, "Multi-Direction Vibration Isolation With Quasi-Zero Stiffness by Employing Geometrical Nonlinearity," *Mech. Syst. Signal Process.*, **62–63**, pp. 149–163.
- [10] Shan, Y., Chen, X., and Wu, W., 2015, "Design of a Miniaturized Pneumatic Vibration Isolator With High-Static-Low-Dynamic Stiffness," *ASME J. Vib. Acoust.*, **137**(4), p. 045001.
- [11] Zheng, Y., Zhang, X., Luo, Y., Yan, B., and Ma, C., 2016, "Design and Experiment of a High-Static-low-Dynamic Stiffness Isolator Using a Negative Stiffness Magnetic Spring," *J. Sound Vib.*, **360**, pp. 31–52.
- [12] Stewart, D., 1965, "A Platform With Six Degrees of Freedom," *Proc. Inst. Mech. Eng.*, **180**(1), pp. 371–386.
- [13] Fichter, E. F., 1986, "A Stewart Platform- Based Manipulator: General Theory and Practical Construction," *Int. J. Rob. Res.*, **5**(2), pp. 157–182.
- [14] Geng, Z. J., and Haynes, L. S., 1994, "Six Degree-of-Freedom Active Vibration Control Using the Stewart Platforms," *IEEE Trans. Control Syst. Technol.*, **2**(1), pp. 45–53.
- [15] Wu, Z., Jing, X., Sun, B., and Li, F., 2016, "A 6DOF Passive Vibration Isolator Using X-Shape Supporting Structures," *J. Sound Vib.*, **380**, pp. 90–111.
- [16] Zheng, Y., Li, Q., Zhang, X., Luo, Y., Zhang, Y., and Xie, S., 2016, "Six-Degrees-of-Freedom Quasi-Zero-Rigidity Vibration Isolation System Based on Stewart Platform," China, Patent Application CN201510395953.
- [17] Yonnet, J. P., 1978, "Passive Magnetic Bearings With Permanent Magnets," *IEEE Trans. Magn.*, **14**(5), pp. 803–805.
- [18] Zhong, W., 1998, *Ferromagnetic Theory (in Chinese)*, China Science Press, Beijing.